

## Accepted Manuscript

Synthesis, biological evaluation and 3D-QSAR study of novel 4,5-dihydro-1*H*-pyrazole thiazole derivatives as BRAF<sup>V600E</sup> inhibitors

Meng-Yue Zhao, Yong Yin, Xiao-Wei Yu, Chetan B. Sangani, Shu-Fu Wang, Ai-Min Lu, Li-Fang Yang, Peng-Cheng Lv, Ming-Guo Jiang, Hai-Liang Zhu

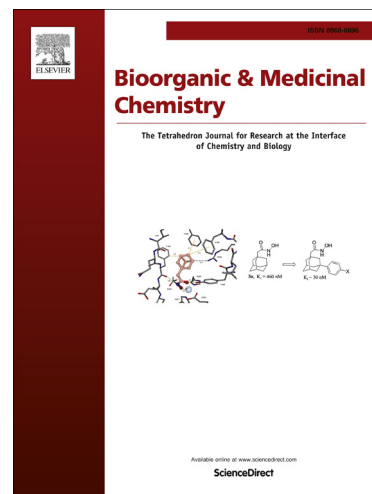
PII: S0968-0896(14)00816-5  
DOI: <http://dx.doi.org/10.1016/j.bmc.2014.11.029>  
Reference: BMC 11918

To appear in: *Bioorganic & Medicinal Chemistry*

Received Date: 21 September 2014  
Revised Date: 19 November 2014  
Accepted Date: 20 November 2014

Please cite this article as: Zhao, M-Y., Yin, Y., Yu, X-W., Sangani, C.B., Wang, S-F., Lu, A-M., Yang, L-F., Lv, P-C., Jiang, M-G., Zhu, H-L., Synthesis, biological evaluation and 3D-QSAR study of novel 4,5-dihydro-1*H*-pyrazole thiazole derivatives as BRAF<sup>V600E</sup> inhibitors, *Bioorganic & Medicinal Chemistry* (2014), doi: <http://dx.doi.org/10.1016/j.bmc.2014.11.029>

This is a PDF file of an unedited manuscript that has been accepted for publication. As a service to our customers we are providing this early version of the manuscript. The manuscript will undergo copyediting, typesetting, and review of the resulting proof before it is published in its final form. Please note that during the production process errors may be discovered which could affect the content, and all legal disclaimers that apply to the journal pertain.



**Synthesis, biological evaluation and 3D-QSAR study of novel 4, 5-dihydro-1H-pyrazole thiazole derivatives as BRAF<sup>V600E</sup> inhibitors**

Meng-Yue Zhao<sup>+a</sup>, Yong Yin<sup>+a</sup>, Xiao-Wei Yu<sup>a</sup>, Chetan B. Sangani<sup>a</sup>, Shu-Fu Wang<sup>a</sup>, Ai-Min Lu<sup>b</sup>,  
Li-Fang Yang<sup>ac</sup>, Peng-Cheng Lv<sup>\*a</sup>, Ming-Guo Jiang<sup>\*ac</sup>, Hai-Liang Zhu<sup>\*a</sup>

<sup>a</sup> State Key Laboratory of Pharmaceutical Biotechnology, Nanjing University, Nanjing 210093,  
People's Republic of China

<sup>b</sup> College of Science, Nanjing Agriculture University, Nanjing 210095, People's Republic of  
China

<sup>c</sup> Guangxi Colleges and Universities Key Laboratory of Utilization of Microbial and Botanical Resources, Guangxi University for nationalities, 530006

<sup>+</sup> These authors contributed equally to this work.

<sup>\*</sup> Corresponding authors. Tel.: +86 25 83592572; Fax: +86 25 83592672.

E-mail address: zhuhl@nju.edu.cn (H.-L. Zhu).

**Abstract**

Many reports implied that the BRAF serine /threonine kinase was mutated in various types of human tumors, which were related with cell growth, survival and differentiation. To provide new therapeutic opportunities, a series of novel 4, 5-dihydro-1*H*-pyrazole derivatives (**6a-10d**) containing thiazole moiety as potential V600E mutant BRAF kinase (BRAF<sup>V600E</sup>) inhibitors were designed and synthesized. All compounds were evaluated *in vitro* for anticancer activities against WM266.4 human melanoma cell line and breast cancer MCF-7 cell line. Compound **10d** displayed the most potential antiproliferative activity with an IC<sub>50</sub> value of 0.12 μM against cell line WM266.4 and 0.16 μM against MCF-7 with positive control Sorafenib. Results of the inhibitory activity against BRAF<sup>V600E</sup> revealed that compound **10d** was bearing the best bioactivity with IC<sub>50</sub> of 0.05 μM as well. On the basis of the result of flow cytometry, with the dose of compound **10d** increasing, more and more cancer cell gradually encountered apoptosis or died, which indicated the compound **10d** could induce remarkable apoptosis of MCF-7 and WM266.4 cells in a dose dependent manner. Furthermore, docking simulation of inhibitor analogues and 3D-QSAR modeling provided potential binding model and further knowledge of pharmacophore.

**Keywords:**4, 5-dihydro-1*H*-pyrazole

Anticancer activity

BRAF<sup>V600E</sup> inhibition

Molecular docking

## 1. Introduction

The Ras/RAF/MEK/ERK mitogen-activated protein kinase (MAPK) signaling pathway plays an important role in the transduction of signals from cell surface receptors to the nucleus, like regulating cell growth, survival, differentiation and proliferation in response to external stimuli (growth factors, cytokines or hormones).<sup>[1]</sup> Phosphorylation of RAF stimulates its serine/threonine activity, triggering and activating the protein kinases MEK and ERK sequentially.<sup>[2]</sup> ERK phosphorylates several transcription factors such as ELK-1 and controls gene expression, cytoskeletal rearrangements and metabolism, causing cell transformation and contributing to tumor initiation and maintenance. Therefore, targeting this pathway, for example through inhibition of BRAF, becomes important in many current human cancer therapeutics approaches.

A number of activating mutations of the BRAF gene have been identified, but the most common change in human cancer is the substitution of a valine for glutamic acid at position 600 (V600E; formally identified as V599E).<sup>[3]</sup> This single mutation accounts for a 500-fold activation compared to the wild type in melanoma, providing cancer cells with proliferation, survival signals, growth and maintenance functions. The large-scale genomic screens have detected that BRAF was mutated in approximately 7% of human tumors,<sup>[4, 5]</sup> colorectal cancer (5–22%),<sup>[4]</sup> papillary thyroid cancer (29–83%),<sup>[4-7]</sup> cholangiocarcinoma (22%),<sup>[8]</sup> and ovarian cancer (30%), especially in melanoma (50–70%).<sup>[9,10]</sup>

The RAF family is serine/threonine kinases, which phosphorylate and activate downstream MEK1/2, including A-RAF, B-RAF and C-RAF (also known as RAF-1) with different biochemical potencies (B-Raf > C-Raf > A-Raf). Several drug development programs in the field of small molecule kinase inhibitors have been initiated, with some representatively marketed compounds such as SB-590885,<sup>[11]</sup> AZ628,<sup>[12]</sup> PLX4032,<sup>[13]</sup> and RAF265.<sup>[14]</sup> A detailed account of the discovery and clinical development of PLX4032, as selective BRAF<sup>V600E</sup> inhibitor that binds to the active conformation of the kinase, has recently been published.<sup>[15,16]</sup> It uses a common scaffold that comprises a terminal aromatic group (phenyl or pyrazole) that fills the allosteric pocket. The relevant compounds were created by the displacement of the DFG loop and an amide linker which couples an aryl group in the hydrophobic pocket to a hinge-binding heterocycle. Linkage via an amide bond would allow for rapid and efficient screening of several

potential hinge-binding groups.<sup>[17,18]</sup> Pyrazole and its derivatives have attracted constant interest over the past decades because of their wide range of pharmacological activities, such as antitumor, anti-inflammatory, antibacterial, analgesic, fungistatic, and anti-hyperglycemic.<sup>[19-21]</sup> SB-590885 has the hottest spots, containing the pyrazolyl ring, which inhibits BRAF<sup>V600E</sup> with a  $K_i$  of 0.16 nmol/L. In consequence, the compounds encompassing pyrazole ring as antineoplastic leads is a reasonable attempt for potential inhibitors of BRAF<sup>V600E</sup>. Based on the studies generalized, thiophene and thiazole group manifest a wide range of pharmaceutical of antibacterial, anti-inflammatory and antiviral property when exposed to the native compounds.<sup>[22,23]</sup> With the development of scientific research, more reports reveal anticancer activities of the compounds containing thiophene and thiazole group,<sup>[24-26]</sup> which inhibits BRAF kinase activity. As a consequence, the combined substructures (thiophene and thiazole group) without wrecking their original effective characteristics, might exhibit synergistic effects to improve anticancer activities<sup>[27-29]</sup>.

In this study, a series of novel pyrazole-based derivatives were recently synthesized as potential anticancer agents targeting BRAF in our group, and some of them demonstrated potential antitumor activity especially about compound **10d** with an  $IC_{50}$  value of 0.12  $\mu$ M against cell line WM266.4 and 0.16  $\mu$ M against MCF-7, which equally shows the most potential antiproliferative activity of apoptosis by flow cytometry experiments. Based on the active data, QSAR model was built to examine the interaction of all the compounds with SB-590885 (2FB8.pdb), and to guide the further study. Docking simulations were performed using the X-ray crystallographic structure of the BRAF in complex with an inhibitor to explore the binding modes of these compounds at the active site.

## 2. Results and Discussion

### 2.1. Chemistry

The synthetic approach of 4,5-dihydro-1*H*-pyrazole derivatives adopted is depicted in Scheme1. First of all, to a solution of thiophene-2-carbaldehyde and different substituted acetophenones, saturated solution of KOH was added slowly. The reaction mixture was stirred until the solids fully formed. Secondly, conduct chalcone derivatives in refluxing KOH ethanol

solution with thiosemicarbazide which leads to the cyclization of the obtained (E)-1-phenyl-3-(thiophen-2-yl)prop-2-en-1-one, eventually to get 3-phenyl-5-(thiophen-2-yl)-4,5-dihydro-1H-pyrazole-1-carbothioamides. Finally, to DMF solution of 3-phenyl-5-(thiophen-2-yl)-4,5-dihydro-1H-pyrazole-1-carbothioamides and 2-Bromoacetophenone, the mixture was allowed to stir. Afterwards, a saturated sodium chloride solution was then slowly added to the reaction flask via a self-equalizing addition funnel. Most commonly, a precipitate formed and was then collected by suction filtration, which was purified by silica gel chromatography after drying out. All of the synthetic compounds gave satisfactory analytical and spectroscopic data, which were in full accordance with their depicted structures.

## 2.2. Bioassay

As described above, the BRAF<sup>V600E</sup> was considered as an important target for the development of small molecule inhibitors in the treatment of human cancers. All compounds were tested against BRAF<sup>V600E</sup> kinases as well as against WM266.4 and MCF-7 cell lines. The results were expressed as concentrations of IC<sub>50</sub> (the half maximal inhibitory concentration of BRAF<sup>V600E</sup> mediated MEK phosphorylation).

Upon investigation of antiproliferative activity of compounds **6a-10d**, it has been observed against WM266.4. Compounds **10d** (IC<sub>50</sub> = 0.12 μM), **7a** (IC<sub>50</sub> = 0.22 μM) and **7b** (IC<sub>50</sub> = 0.17 μM) showed most potent activity as compared to other compounds of the series and less comparable to the positive control Sorafenib (IC<sub>50</sub> = 0.06 μM). While performed against MCF-7 compounds **10d** (IC<sub>50</sub> = 0.16 μM) showed most potent activity; in addition, compounds **7d** (IC<sub>50</sub> = 1.33 μM) **9c** (IC<sub>50</sub> = 0.68 μM) and **10b** (IC<sub>50</sub> = 0.19 μM) showed good activity as compared to other compounds of the series and comparable to the positive control Sorafenib (IC<sub>50</sub> = 0.19 μM).

As shown in Table 1, inhibitory activity conducted against BRAF<sup>V600E</sup> kinases, compound **10d** (IC<sub>50</sub> = 0.05 μM) displayed the most potent inhibitory activity. As well, compounds **7b** (IC<sub>50</sub> = 0.67 μM), **8a** (IC<sub>50</sub> = 0.56 μM), **8c** (IC<sub>50</sub> = 0.11 μM) and **9c** (IC<sub>50</sub> = 0.08 μM) showed excellent activity as compared to other compounds of the series and less to the positive control Sorafenib (IC<sub>50</sub> = 0.03 μM).

Structure activity relationship (SAR) was carried out of BRAF<sup>V600E</sup> kinase. According to the activity data, it has been observed that the change in R<sub>1</sub> and R<sub>2</sub> substitution may lead to change in the activity against employed cancer cells as well as BRAF<sup>V600E</sup> kinase. Compounds containing R<sub>1</sub>=Cl and R<sub>2</sub>=CF<sub>3</sub> (Compound **10d**) have proved as most effective members against BRAF<sup>V600E</sup> kinase and two cancer cell lines WM266.4 and MCF-7. Against BRAF<sup>V600E</sup> kinase, compounds **6d** (IC<sub>50</sub> =10.90μM) and **8d** (IC<sub>50</sub> =6.18μM) owning a substitution at R<sub>1</sub> position is electron releasing group (R<sub>1</sub> = OCH<sub>3</sub>, CH<sub>3</sub>) but when it is replaced by electron withdrawing group (R<sub>1</sub> = F, Cl, Br) in compounds **7d** (IC<sub>50</sub> =1.01 μM), **9d** (IC<sub>50</sub> =2.09 μM) and **10d** (IC<sub>50</sub> =0.05 μM) the activity increases. The activity in decreasing order for R<sub>1</sub> substitution is Cl>Br>F>CH<sub>3</sub>>OCH<sub>3</sub> and for R<sub>2</sub> substitution is CF<sub>3</sub>>H>OCH<sub>3</sub>>Br, while against for cancer cell lines WM266.4 and MCF-7 the activity in increasing order for R<sub>1</sub> substitution is OCH<sub>3</sub><CH<sub>3</sub><Br<F<Cl and for R<sub>2</sub> substitution is OCH<sub>3</sub><H<Br<CF<sub>3</sub>. The above results indicated that the pyrazolyl core, as well as the phenyl thiazole motif, plays an important role in the BRAF<sup>V600E</sup> inhibition. The activity of the compounds was slightly influenced by the changes of substituents on the benzene thiazole rings. Moreover, reviewing and comparing the activity data, it is worthy to mention that the anticancer activity and inhibition against BRAF<sup>V600E</sup> kinases of the target compounds depends not only on the bicyclic heteroaromatic pharmacophore, but also on the nature of the substituents.

According to the apoptosis expression by flow cytometry, the 4, 5-dihydro-1*H*-pyrazole derivatives show cell proliferation activity in another way. To examine whether compound **10d** can induce apoptosis of MCF-7 and WM266.4, flow cytometry method of operation was applied. We observed an obvious reduction in 1 and 3 μM concentration respectively. In contrast, no significant change was seen in control group. When the concentration increased to 3 μM, apoptosis emerges more evidently in Fig. 1

### 2.3. Molecular docking

To gain a better understanding of the potency of the synthesized compounds and guide further SAR studies, we proceeded to examine the interaction of the 4, 5-dihydro-1*H*-pyrazole derivatives with the BRAF<sup>V600E</sup> crystal structure (PDB code: 2FB8). The molecular docking was performed by inserting the compound into the SB-590885 binding site of BRAF<sup>V600E</sup>. All

docking runs were performed by Discovery Studio 3.5 (Discovery Studio 3.5, Accelrys, Inc., San Diego, CA).

Residues within a distance of 10 Å around the BRAF<sup>V600E</sup> inhibitor SB-590885 were isolated for the construction of the grid for docking screening. This grid was large enough to include every residue of the BRAF<sup>V600E</sup> kinase ATP binding pocket. The binding models of compound **10d** and BRAF<sup>V600E</sup> are depicted in Fig. 2 and Fig. 3 and binding energy of compounds **6a-10d** with BRAF<sup>V600E</sup> demonstrated the possibility of inhibition in Table 2. The amino acid residues which interact with BRAF<sup>V600E</sup> are labeled. In the binding mode, compound **10d** binds to BRAF<sup>V600E</sup> via two  $\pi$ - $\pi$  interaction. Among them is one  $\pi$ - $\pi$  interaction are formed between the thiazole rings of compound **10d** and PHE583 having distance = 5.2 Å and second  $\pi$ - $\pi$  interaction are formed between the benzene rings of compound **10d** and HIS539 having distance = 5.2 Å. Extensive hydrophobic interactions are formed between compound **10d** and residues VAL471, ALA481, LYS483, LEU514, ILE527, PHE583, suggesting that the introduction of the hydrophobic group from the phenyl isocyanate has enhanced the affinity of the receptor BRAF<sup>V600E</sup> for the ligand compound **10d**. This molecular docking result, along with the enzyme assay data, suggests that compound **10d** is a potential inhibitor of BRAF<sup>V600E</sup>.

#### 2.4. 3D QSAR model

To evaluate the synthesized compounds 4, 5-dihydro-1*H*-pyrazole derivatives as BRAF inhibitors and to explore more potent inhibitors, 3D QSAR models were built using the Create 3D QSAR protocol of Discovery Studio 3.5. In this study, 20 compounds bearing 4, 5-dihydro-1*H*-pyrazole core with definite IC<sub>50</sub> values were selected as the model dataset. By convention, the pIC<sub>50</sub> scale (-log IC<sub>50</sub>), which higher values indicate exponentially greater potency, which is used as a method to measure inhibitory activity. The training and test set was chosen by the Diverse Molecules method in Discovery Studio. Because a good alignment is very important for the analysis of molecular fields, we applied the CDOCKER protocol to explore each molecule with the lowest energy before alignment conformation. 4, 5-dihydro-1*H*-pyrazole was selected as substructure to build the alignment conformation before building the QSAR model.

The correlation coefficient  $r^2$ , between the observed and predicted activity of the training set and test set, proved that the built QSAR model was acceptable. Predicted pIC<sub>50</sub> values and

residual errors for the 20 compounds by this QSAR model are given in Table 3. The good agreement between predicted and experimental pIC<sub>50</sub> values for both test sets and training sets is shown in Fig. 4.

The molecules aligned with the iso-surfaces of the 3D-QSAR model coefficients on van der Waals grids (Fig. 5a) and electro-static potential grids (Fig. 5b) were also listed. The electrostatic map has red contours around the regions where high electron density (negative charge) is expected to increase activity, and blue contours around areas where low electron density (partial positive charge) is expected to increase activity. Similarly, the steric map has areas where steric bulk is predicted to increase (green) or decrease (yellow) activity.

According to the maps, it is suggested that the compound with high negative charged and small R<sub>1</sub> group, would show higher activity, attesting that chlorine substituent from being a better choice. Whereas, a low negative charged and bulky R<sub>2</sub> group would help obtain sound activity, validating the trifluoromethyl substituent could be more effective. As a result, data summarized above demonstrate that compound **10d**, the most potent BRAF inhibitor (IC<sub>50</sub> against WM266.4=0.12 μM, IC<sub>50</sub> against MCF-7=0.16 μM), containing favored substituents has an outstanding activity. The 3D QSAR models fit the inhibitory activity well, which thus provides us with a direction for further modification.

### 3. Conclusion

In this study, a series of 4, 5-dihydropyrazole derivatives, containing thiazole and thiophene moiety, as potential V600E mutant BRAF kinase (BRAF<sup>V600E</sup>) inhibitors were designed and synthesized. According to the biological active data, it could be concluded that majority of the compounds showed effective BRAF<sup>V600E</sup> inhibitory activity and antiproliferative activity against WM266.4 and MCF-7 cell lines. Among these compounds, **10d** showed the most potent BRAF<sup>V600E</sup> inhibitory activity (IC<sub>50</sub> = 0.05 μM) and antiproliferative activity (IC<sub>50</sub> = 0.12 μM for WM266.4 and IC<sub>50</sub> = 0.16 μM for MCF-7). From the result of flow cytometry, more and more cancer cell gradually encountered apoptosis or died with the dose of compound **10d** increasing, which indicated the compound **10d** could induce remarkable apoptosis of MCF-7 and WM266.4 cells. Molecular docking studies provided further insight into interactions between the BRAF<sup>V600E</sup> protein and its ligand. After analyzing the binding model of compound **10d** with BRAF, we

found that one  $\pi$ - $\pi$  interaction and the hydrophobic interactions with the protein residues in the ATP binding site might play essential roles in its BRAF<sup>V600E</sup> inhibition and antiproliferative activity. Therefore, it can be concluded that compound **10d** as well as the other pyrazole derivatives, containing effective thiazole and thiophene pharmacophore, are promising subjects for further study as potential anticancer agents. The results of this study might help with the search for a promising BRAF<sup>V600E</sup> inhibitor with potent activity.

## 4. Experimental

### 4.1. Materials and measurements

All chemicals and reagents used in the current study were of analytical grade. Melting points (uncorrected) were determined on an XT4 MP apparatus (Taikang Corp., Beijing, China). All the <sup>1</sup>H NMR and <sup>13</sup>C NMR spectra were recorded on a Bruker DPX400 model Spectrometer in DMSO-*d*<sub>6</sub> and chemical shifts were reported in ppm (d). FTIR spectra (KBr) were run on a Nexus 870 FT-IR spectrophotometer. ESI-MS spectra were recorded on a Mariner System 5304 mass spectrometer. Elemental analyses were performed on a CHN-O-Rapid instrument. TLC was performed on the glass backed silica gel sheets (Silica Gel 60 GF254) and visualized in UV light (254 nm).

### 4.2. General procedure for synthesis of chalcones

To a stirred solution of acetophenone derivatives (10 mmol) and a thiophene-2-carbaldehyde (10 mmol) in ethanol (30 mL), a saturated solution of KOH (6 mol/4 L) was added slowly. The reaction mixture was stirred until the solids fully formed. The products were filtrated and washed carefully with ice water and cool ethanol, then purified by crystallization from ethanol in refrigerator to give chalcones.

### 4.3. General procedure for synthesis of 3-phenyl-5-(thiophen-2-yl)-4,5-dihydro-1H-pyrazole-1-carbothioamide

To ethanol (45 mL) solution of equimolar quantities thiosemicarbazide (15 mmol) and chalcone ketones (15 mmol) obtained from step one, KOH (15-18mmol) was slowly added with stirring. The mixture was refluxed by 2 hours at 80°C. After completion of the reaction, the contents were cooled. The product was filtered and purified by recrystallization from ethanol.

#### 4.4. General procedure for synthesis of 4-phenyl-2-(3-phenyl-5-(thiophen-2-yl)-4,5-dihydro-1H-pyrazol-1-yl)thiazole

To DMF (45mL) solution of 3-phenyl-5-(thiophen-2-yl)-4,5-dihydro-1H-pyrazole-1-carbothioamide (10 mmol) and 2-Bromoacetophenone (10 mmol), the mixture was allowed to stir for 3 hours at 25 °C. After completion of the reaction, a 40 mL aliquot of a saturated sodium chloride solution was then slowly added to the reaction flask via a self-equalizing addition funnel. Most commonly, a precipitate formed and was then collected by suction filtration. After drying at room temperature, the residue was purified by silica gel chromatography (PE/EtOAc=10:1) to afford pure compounds.

##### 4.4.1. 4-(4-Bromophenyl)-2-(3-(4-methoxyphenyl)-5-(thiophen-2-yl)-4,5-dihydro-1H-pyrazol-1-yl)thiazole (6a).

Yield 76%; mp. 211-213 °C. <sup>1</sup>H NMR (400 MHz, DMSO): δ 3.50-3.56 (m, 1H, CH<sub>2</sub>); 3.82 (s, 3H, OCH<sub>3</sub>); 3.98-4.06 (m, 1H, CH<sub>2</sub>); 5.95-5.99 (m, 1H, CH); 6.99 (t, J = 3.60 Hz, 1H, ArH); 7.04 (d, J = 3.60 Hz, 1H, ArH); 7.06 (d, J = 3.60 Hz, 1H, ArH); 7.24 (s, 1H, ArH); 7.44 (d, J = 3.20 Hz, 2H, ArH); 7.59 (d, J = 8.40 Hz, 2H, ArH); 7.77 (t, J = 17.70 Hz, 4H, ArH). ESI-MS: 497.39 (C<sub>23</sub>H<sub>19</sub>BrN<sub>3</sub>OS<sub>2</sub>, [M+H]<sup>+</sup>). Anal. Calcd for C<sub>23</sub>H<sub>18</sub>BrN<sub>3</sub>OS<sub>2</sub>: C, 55.65; H, 3.65; N, 8.46; Found: C, 55.45; H, 3.45; N, 8.56.

##### 4.4.2. 2-(3-(4-Methoxyphenyl)-5-(thiophen-2-yl)-4,5-dihydro-1H-pyrazol-1-yl)-4-phenylthiazole (6b).

Yield 69%; mp. 174-176 °C. <sup>1</sup>H NMR (400 MHz, DMSO): δ 3.49-3.55 (m, 1H, CH<sub>2</sub>); 3.82 (s, 3H, OCH<sub>3</sub>); 3.98-4.06 (m, 1H, CH<sub>2</sub>); 5.95-5.99 (m, 1H, CH); 6.99 (t, J = 3.60 Hz, 1H, ArH); 7.04 (d, J = 3.60 Hz, 1H, ArH); 7.06 (d, J = 3.60 Hz, 1H, ArH); 7.25 (d, J=3.50 Hz, 1H, ArH); 7.29 (d, J = 7.30 Hz, 1H, ArH); 7.37 (t, J = 13.20 Hz, 3H, ArH); 7.41-7.45 (m, 1H, ArH); 7.76

(d,  $J = 8.80$  Hz, 2H, ArH); 7.82-7.84 (d,  $J = 7.20$  Hz, 2H, ArH). ESI-MS: 418.58 ( $C_{23}H_{20}N_3OS_2$ ,  $[M+H]^+$ ). Anal. Calcd for  $C_{23}H_{19}N_3OS_2$ : C, 66.16; H, 4.59; N, 10.06; Found: C, 66.11; H, 4.49; N, 10.16.

**4.4.3. 4-(4-Methoxyphenyl)-2-(3-(4-methoxyphenyl)-5-(thiophen-2-yl)-4,5-dihydro-1H-pyrazol-1-yl)thiazole (6c).**

Yield 59%; mp. 198-201 °C.  $^1H$  NMR (400 MHz, DMSO):  $\delta$  3.35-3.54 (m, 1H,  $CH_2$ ); 3.77 (s, 3H,  $OCH_3$ ); 3.82 (s, 3H,  $OCH_3$ ); 3.98-4.05 (m, 1H,  $CH_2$ ); 5.93-5.98 (m, 1H, CH); 6.94 (d,  $J = 8.80$  Hz, 2H, ArH); 6.99 (t,  $J = 3.60$  Hz, 1H, ArH); 7.04 (d,  $J = 3.60$  Hz, 1H, ArH); 7.06 (d,  $J = 3.60$  Hz, 1H, ArH); 7.18 (s, 1H, ArH); 7.24 (d,  $J = 1.20$  Hz, 1H, ArH); 7.43-7.45 (m, 1H, ArH); 7.76 (d,  $J = 8.00$  Hz, 4H, ArH). ESI-MS: 448.48 ( $C_{24}H_{22}N_3O_2S_2$ ,  $[M+H]^+$ ). Anal. Calcd for  $C_{24}H_{21}N_3O_2S_2$ : C, 64.40; H, 4.73; N, 9.39; Found: C, 64.20; H, 4.63; N, 9.45.

**4.4.4. 2-(3-(4-Methoxyphenyl)-5-(thiophen-2-yl)-4,5-dihydro-1H-pyrazol-1-yl)-4-(4-(trifluoromethyl)phenyl)thiazole (6d).**

Yield 49%; mp. 208-209 °C.  $^1H$  NMR (400 MHz, DMSO):  $\delta$  3.51-3.58 (m, 1H,  $CH_2$ ); 3.82 (d,  $J = 8.40$  Hz, 3H,  $OCH_3$ ); 4.00-4.07 (m, 1H,  $CH_2$ ); 5.98-6.02 (m, 1H, CH); 6.98-7.00 (m, 1H, ArH); 7.05 (d,  $J = 3.60$  Hz, 1H, ArH); 7.07 (d,  $J = 3.60$  Hz, 1H, ArH); 7.26 (d,  $J = 10.80$  Hz, 1H, ArH); 7.44 (d,  $J = 4.00$  Hz, 1H, ArH); 7.62 (d,  $J = 11.60$  Hz, 1H, ArH); 7.75-7.78 (m, 4H, ArH); 8.03 (d,  $J = 2.00$  Hz, 2H, ArH). ESI-MS: 486.61 ( $C_{24}H_{19}F_3N_3OS_2$ ,  $[M+H]^+$ ). Anal. Calcd for  $C_{24}H_{18}F_3N_3OS_2$ : C, 59.37; H, 3.74; N, 8.65; Found: C, 59.17; H, 3.72; N, 8.45.

**4.4.5. 4-(4-Bromophenyl)-2-(3-(4-fluorophenyl)-5-(thiophen-2-yl)-4,5-dihydro-1H-pyrazol-1-yl)thiazole (7a).**

Yield 67%; mp. 199-201 °C.  $^1H$  NMR (400 MHz, DMSO):  $\delta$  3.55-3.61 (m, 1H,  $CH_2$ ); 4.02-4.10 (m, 1H,  $CH_2$ ); 6.00-6.04 (m, 1H, CH); 7.00 (t,  $J = 8.40$  Hz, 1H, ArH); 7.26 (d,  $J = 0.80$  Hz, 1H, ArH); 7.35 (t,  $J = 17.20$  Hz, 2H, ArH); 7.45 (d,  $J = 7.60$  Hz, 2H, ArH); 7.60 (d,  $J = 8.40$  Hz, 2H, ArH); 7.78-7.80 (d,  $J = 8.40$  Hz, 2H, ArH); 7.86-7.90 (m, 2H, ArH). ESI-MS: 485.44 ( $C_{22}H_{16}BrFN_3S_2$ ,  $[M+H]^+$ ). Anal. Calcd for  $C_{22}H_{15}BrFN_3S_2$ : C, 54.55; H, 3.12; N, 8.67; Found: C, 54.45; H, 3.21; N, 8.68.

**4.4.6. 2-(3-(4-Fluorophenyl)-5-(thiophen-2-yl)-4,5-dihydro-1H-pyrazol-1-yl)-4-phenylthiazole (7b).**

Yield 54%; mp. 156-157 °C. <sup>1</sup>H NMR (400 MHz, DMSO): δ 3.53-3.59 (m, 1H, CH<sub>2</sub>); 4.01-4.08 (m, 1H, CH<sub>2</sub>); 5.99-6.03 (m, 1H, CH); 7.00 (t, *J* = 8.40 Hz, 1H, ArH); 7.26-7.32 (m, 2H, ArH); 7.34 (s, 5H, ArH); 7.37-7.45 (m, 1H, ArH); 7.83-7.89 (m, 4H, ArH). ESI-MS: 406.53 (C<sub>22</sub>H<sub>17</sub>FN<sub>3</sub>S<sub>2</sub>, [M+H]<sup>+</sup>). Anal. Calcd for C<sub>22</sub>H<sub>16</sub>FN<sub>3</sub>S<sub>2</sub>: C, 65.16; H, 3.98; N, 10.36; Found: C, 65.25; H, 3.79; N, 10.46.

**4.4.7. 2-(3-(4-Fluorophenyl)-5-(thiophen-2-yl)-4,5-dihydro-1H-pyrazol-1-yl)-4-(4-methoxyphenyl)thiazole (7c).**

Yield 65%; mp. 181-183 °C. <sup>1</sup>H NMR (400 MHz, DMSO): δ 3.5-3.59 (m, 1H, CH<sub>2</sub>); 3.79 (s, 3H, OCH<sub>3</sub>); 4.02-4.09 (m, 1H, CH<sub>2</sub>); 5.99-6.03 (m, 1H, CH); 6.97 (t, *J* = 22.80 Hz, 3H, ArH); 7.20 (s, 1H, ArH); 7.26(s, 1H, ArH); 7.35 (t, *J* = 8.40 Hz, 2H, ArH); 7.45(d, *J* = 4.80 Hz, 1H, ArH); 7.77 (d, *J* = 8.40 Hz, 2H, ArH); 7.88 (t, *J* = 13.20 Hz, 2H, ArH). ESI-MS: 436.44 (C<sub>23</sub>H<sub>19</sub>FN<sub>3</sub>OS<sub>2</sub>, [M+H]<sup>+</sup>). Anal. Calcd for C<sub>23</sub>H<sub>18</sub>FN<sub>3</sub>OS<sub>2</sub>: C, 63.43; H, 4.17; N, 9.65; Found: C, 63.53; H, 4.23; N, 9.85.

**4.4.8. 2-(3-(4-Fluorophenyl)-5-(thiophen-2-yl)-4,5-dihydro-1H-pyrazol-1-yl)-4-(4-(trifluoromethyl)phenyl)thiazole (7d).**

Yield 52%; mp. 198-200 °C. <sup>1</sup>H NMR (400 MHz, DMSO): δ 3.55-3.61 (m, 1H, CH<sub>2</sub>); 4.02-4.10 (m, 1H, CH<sub>2</sub>); 6.01-6.05 (m, 1H, CH); 7.00 (t, *J* = 8.40 Hz, 1H, Ar-H); 7.27 (d, *J* = 3.20 Hz, 1H, ArH); 7.43 (t, *J* = 16.80 Hz, 2H, ArH); 7.44 (d, *J* = 4.80 Hz, 1H, ArH); 7.63 (d, *J* = 14.80 Hz, 1H, ArH); 7.75 (d, *J* = 8.00 Hz, 2H, ArH); 7.78 (d, *J* = 24.00 Hz, 2H, ArH); 8.04(d, *J* = 8.10 Hz, 2H, ArH). ESI-MS: 474.49 (C<sub>23</sub>H<sub>16</sub>F<sub>4</sub>N<sub>3</sub>S<sub>2</sub>, [M+H]<sup>+</sup>). Anal. Calcd for C<sub>23</sub>H<sub>15</sub>F<sub>4</sub>N<sub>3</sub>S<sub>2</sub>: C, 58.34; H, 3.19; N, 8.87; Found: C, 58.45; H, 3.32; N, 8.81.

**4.4.9. 4-(4-Bromophenyl)-2-(5-(thiophen-2-yl)-3-p-tolyl-4,5-dihydro-1H-pyrazol-1-yl)thiazole (8a).**

Yield 72%; mp. 209-210 °C. <sup>1</sup>H NMR (400 MHz, DMSO): δ 2.37 (s, 3H, CH<sub>3</sub>); 3.51-3.56 (m, 23.6 Hz, 1H, CH<sub>2</sub>); 3.99-4.07 (m, 1H, CH<sub>2</sub>); 5.97-6.02 (m, 1H, CH); 6.98-7.00 (m, 1H, ArH); 7.25 (d, *J* = 3.60 Hz, 1H, ArH); 7.31 (d, *J* = 8.00 Hz, 2H, ArH); 7.45 (t, *J* = 8.00 Hz, 2H, ArH); 7.59 (d, *J* = 15.80 Hz, 2H, ArH); 7.71 (d, *J* = 8.10 Hz, 2H, ArH); 7.78 (d, *J* = 8.60 Hz, 2H, ArH). ESI-MS: 481.49 (C<sub>23</sub>H<sub>19</sub>BrN<sub>3</sub>S<sub>2</sub>, [M+H]<sup>+</sup>). Anal. Calcd for C<sub>23</sub>H<sub>18</sub>BrN<sub>3</sub>S<sub>2</sub>: C, 57.50; H, 3.78; N, 8.75; Found: C, 57.60; H, 3.88; N, 8.78.

**4.4.10. 4-Phenyl-2-(5-(thiophen-2-yl)-3-p-tolyl-4,5-dihydro-1H-pyrazol-1-yl)thiazole(8b).**

Yield 61%; mp. 190-192 °C. <sup>1</sup>H NMR (400 MHz, DMSO): δ 2.37 (s, 3H, CH<sub>3</sub>); 3.50-3.56 (m, 1H, CH<sub>2</sub>); 3.99-4.06 (m, 1H, CH<sub>2</sub>); 5.97-6.01 (m, 1H, CH); 6.99 (t, *J* = 8.40 Hz, 1H, ArH); 7.25-7.30 (m, 4H, ArH); 7.32 (s, 3H, ArH); 7.37-7.45 (m, 1H, ArH). 7.71 (d, *J* = 8.00 Hz, 2H, ArH); 7.83-7.84 (d, *J* = 7.60 Hz, 2H, ArH). ESI-MS: 402.59 (C<sub>23</sub>H<sub>20</sub>N<sub>3</sub>S<sub>2</sub>, [M+H]<sup>+</sup>). Anal. Calcd for C<sub>23</sub>H<sub>19</sub>N<sub>3</sub>S<sub>2</sub>: C, 68.80; H, 4.77; N, 10.46; Found: C, 68.70; H, 4.79; N, 10.66.

**4.4.11. 4-(4-Methoxyphenyl)-2-(5-(thiophen-2-yl)-3-p-tolyl-4,5-dihydro-1H-pyrazol-1-yl)thiazole (8c).**

Yield 48%; mp. 198-200 °C. <sup>1</sup>H NMR (400 MHz, DMSO): δ 2.37 (s, 3H, CH<sub>3</sub>); 3.49-3.55 (m, 1H, CH<sub>2</sub>); 3.77 (s, 3H, OCH<sub>3</sub>); 3.99-4.06 (m, 1H, CH<sub>2</sub>); 5.96-6.00 (m, 1H, CH); 6.94-7.00 (m, 3H, ArH); 7.19 (s, 1H, ArH); 7.25 (d, *J* = 3.20 Hz, 1H, ArH); 7.31 (d, *J* = 4.00 Hz, 2H, ArH); 7.44 (d, *J* = 17.20 Hz, 1H, ArH); 7.70-7.77 (m, 4H, ArH). ESI-MS: 432.61(C<sub>24</sub>H<sub>22</sub>N<sub>3</sub>OS<sub>2</sub>, [M+H]<sup>+</sup>). Anal. Calcd for C<sub>24</sub>H<sub>21</sub>N<sub>3</sub>OS<sub>2</sub>: C, 66.79; H, 4.90; N, 9.74; Found: C, 66.89; H, 4.95; N, 9.84.

**4.4.12. 2-(5-(Thiophen-2-yl)-3-p-tolyl-4,5-dihydro-1H-pyrazol-1-yl)-4-(4-(trifluoromethyl)phenyl)thiazole (8d).**

Yield 67%; mp. 208-209 °C. <sup>1</sup>H NMR (400 MHz, DMSO): δ 2.35 (s, 3H, CH<sub>3</sub>); 3.56-3.58 (d, *J* = 6.00 Hz, 1H, CH<sub>2</sub>); 4.00-4.07 (m, 1H, CH<sub>2</sub>); 5.99-6.03 (m, 1H, CH); 6.98-7.00 (m, 1H, ArH); 7.26 (d, *J* = 3.20 Hz, 1H, ArH), 7.31 (d, *J* = 8.00 Hz, 2H, ArH); 7.43-7.45 (m, 1H, ArH); 7.62 (s, 1H, ArH); 7.71 (d, *J* = 8.00 Hz, 2H, ArH); 7.75 (d, *J* = 8.40 Hz, 2H, ArH); 8.04 (d, *J* =

8.00 Hz, 2H, ArH). ESI-MS: 470.60 (C<sub>24</sub>H<sub>19</sub>F<sub>3</sub>N<sub>3</sub>S<sub>2</sub>, [M+H]<sup>+</sup>). Anal. Calcd for C<sub>24</sub>H<sub>18</sub>F<sub>3</sub>N<sub>3</sub>S<sub>2</sub>: C, 61.39; H, 3.86; N, 8.95; Found: C, 61.59; H, 3.66; N, 8.96.

**4.4.13. 4-(4-Bromophenyl)-2-(3-(4-bromophenyl)-5-(thiophen-2-yl)-4,5-dihydro-1H-pyrazol-1-yl)thiazole (9a).**

Yield 59%; mp. 219-201 °C. <sup>1</sup>H NMR (400 MHz, DMSO): δ 3.55-3.61 (m, 1H, CH<sub>2</sub>); 4.02-4.09 (m, 1H, CH<sub>2</sub>); 6.03-6.07 (m, 1H, CH); 7.00 (t, *J* = 8.40 Hz, 1H, ArH); 7.27-7.28 (d, *J* = 3.20 Hz, 1H, ArH); 7.44-7.46 (d, *J* = 5.20 Hz, 1H, ArH); 7.64 (s, 1H, ArH); 7.70-7.72 (d, *J* = 8.40 Hz, 2H, ArH); 7.75-7.77 (d, *J* = 8.80 Hz, 4H, ArH); 8.03-8.05 (d, *J* = 8.10 Hz, 2H, ArH). ESI-MS: 546.38 (C<sub>22</sub>H<sub>16</sub>Br<sub>2</sub>N<sub>3</sub>S<sub>2</sub>, [M+H]<sup>+</sup>). Anal. Calcd for C<sub>22</sub>H<sub>15</sub>Br<sub>2</sub>N<sub>3</sub>S<sub>2</sub>: C, 48.46; H, 2.77; N, 7.71; Found: C, 48.56; H, 2.84; N, 7.81.

**4.4.14. 2-(3-(4-Bromophenyl)-5-(thiophen-2-yl)-4,5-dihydro-1H-pyrazol-1-yl)-4-phenylthiazole (9b).**

Yield 66%; mp. 180-182 °C. <sup>1</sup>H NMR (400 MHz, DMSO): δ 3.53-3.59 (m, 1H, CH<sub>2</sub>); 4.00-4.07 (m, 1H, CH<sub>2</sub>); 6.00-6.05 (m, 1H, CH); 6.99-7.01 (m, 1H, ArH); 7.26-7.30 (m, 2H, ArH); 7.39 (t, *J* = 15.20 Hz, 3H, ArH); 7.44-7.46 (m, 1H, ArH); 7.69-7.76 (m, 4H, ArH); 7.84 (t, *J* = 8.40 Hz, 2H, ArH). ESI-MS: 467.48 (C<sub>22</sub>H<sub>17</sub>BrN<sub>3</sub>S<sub>2</sub>, [M+H]<sup>+</sup>). Anal. Calcd for C<sub>22</sub>H<sub>16</sub>BrN<sub>3</sub>S<sub>2</sub>: C, 56.65; H, 3.46; N, 9.01; Found: C, 56.75; H, 3.49; N, 9.00.

**4.4.15. 2-(3-(4-Bromophenyl)-5-(thiophen-2-yl)-4,5-dihydro-1H-pyrazol-1-yl)-4-(4-methoxyphenyl)thiazole (9c).**

Yield 45%; mp. 196-198 °C. <sup>1</sup>H NMR (400 MHz, DMSO): δ 3.51-3.57 (m, 1H, CH<sub>2</sub>); 3.77 (s, 3H, OCH<sub>3</sub>); 3.95-4.07 (m, 1H, CH<sub>2</sub>); 5.99-6.03 (m, 1H, CH); 6.95 (d, *J* = 8.40 Hz, 2H, ArH); 6.99 (t, *J* = 8.40 Hz, 1H, ArH); 7.20 (s, 1H, ArH); 7.25-7.26 (d, *J* = 3.20 Hz, 1H, ArH); 7.44 (d, *J* = 5.20 Hz, 1H, ArH); 7.68-7.71 (d, *J* = 7.60 Hz, 2H, ArH); 4.09 (s, 4H, ArH). ESI-MS: 497.49 (C<sub>23</sub>H<sub>19</sub>BrN<sub>3</sub>OS<sub>2</sub>, [M+H]<sup>+</sup>). Anal. Calcd for C<sub>23</sub>H<sub>18</sub>BrN<sub>3</sub>OS<sub>2</sub>: C, 55.65; H, 3.65; N, 8.46; Found: C, 55.75; H, 3.68; N, 8.52.

**4.4.16. 2-(3-(4-Bromophenyl)-5-(thiophen-2-yl)-4,5-dihydro-1H-pyrazol-1-yl)-4-(4-(trifluoromethyl)phenyl)thiazole (9d).**

Yield 49%; mp. 196-197 °C. <sup>1</sup>H NMR (400 MHz, DMSO): δ 3.52-3.58 (m, 1H, CH<sub>2</sub>); 3.99-4.07 (m, 1H, CH<sub>2</sub>); 5.99-6.04 (m, 1H, CH); 6.94-7.01 (m, 3H, ArH); 7.25 (t, *J* = 19.20 Hz, 2H, ArH); 7.45 (d, *J* = 4.80 Hz, 1H, ArH); 7.69-7.77 (m, 6H, ArH). ESI-MS: 535.51 (C<sub>23</sub>H<sub>16</sub>BrF<sub>3</sub>N<sub>3</sub>S<sub>2</sub>, [M+H]<sup>+</sup>). Anal. Calcd for C<sub>23</sub>H<sub>15</sub>BrF<sub>3</sub>N<sub>3</sub>S<sub>2</sub>: C, 51.69; H, 2.83; N, 7.86; Found: C, 51.79; H, 2.93; N, 7.90.

**4.4.17. 4-(4-Bromophenyl)-2-(3-(4-chlorophenyl)-5-(thiophen-2-yl)-4,5-dihydro-1H-pyrazol-1-yl)thiazole (10a).**

Yield 54%; mp. 218-220 °C. <sup>1</sup>H NMR (400 MHz, DMSO): δ 3.54-3.60 (m, 1H, CH<sub>2</sub>); 4.05-4.078 (m, 1H, CH<sub>2</sub>); 6.01-6.05 (m, 1H, CH); 6.93-7.00 (m, 1H, ArH); 7.26 (d, *J* = 3.20 Hz, 1H, ArH); 7.45 (t, *J* = 14.00 Hz, 2H, ArH); 7.58 (t, *J* = 17.30 Hz, 4H, ArH); 7.77-7.84 (m, 4H, ArH). ESI-MS: 501.91 (C<sub>22</sub>H<sub>16</sub>ClN<sub>3</sub>S<sub>2</sub>, [M+H]<sup>+</sup>). Anal. Calcd for C<sub>22</sub>H<sub>15</sub>ClN<sub>3</sub>S<sub>2</sub>: C, 52.76; H, 3.02; N, 8.39; Found: C, 52.79; H, 3.02; N, 8.30.

**4.4.18. 2-(3-(4-Chlorophenyl)-5-(thiophen-2-yl)-4,5-dihydro-1H-pyrazol-1-yl)-4-phenylthiazole (10b).**

Yield 43 %; mp. 160-163 °C. <sup>1</sup>H NMR (400 MHz, DMSO): δ 3.54-3.60 (m, 1H, CH<sub>2</sub>); 4.01-4.08 (m, 1H, CH<sub>2</sub>); 6.01-6.05 (m, 1H, CH); 6.99-7.01 (m, 1H, ArH); 7.26-7.30 (m, 2H, ArH); 7.37-7.42 (m, 3H, ArH); 7.46 (t, *J* = 12.00 Hz, 1H, ArH); 7.58 (t, *J* = 17.20 Hz, 2H, ArH); 7.82-7.84 (m, 4H, ArH). ESI-MS: 422.87 (C<sub>22</sub>H<sub>17</sub>ClN<sub>3</sub>S<sub>2</sub>, [M+H]<sup>+</sup>). Anal. Calcd for C<sub>22</sub>H<sub>16</sub>ClN<sub>3</sub>S<sub>2</sub>: C, 62.62; H, 3.82; N, 9.96; Found: C, 62.72; H, 3.89; N, 9.99.

**4.4.19. 2-(3-(4-Chlorophenyl)-5-(thiophen-2-yl)-4,5-dihydro-1H-pyrazol-1-yl)-4-(4-methoxyphenyl)thiazole (10c).**

Yield 51%; mp. 185-186 °C. <sup>1</sup>H NMR (400 MHz, DMSO): δ 3.52-3.58 (m, 1H, CH<sub>2</sub>); 3.77 (s, 3H, OCH<sub>3</sub>); 4.00-4.07 (m, 1H, CH<sub>2</sub>); 5.99-6.04 (m, 1H, CH); 6.94-7.01 (m, 3H, ArH); 7.25 (t, *J* = 18.00 Hz, 2H, ArH); 7.45(d, *J* = 4.40 Hz, 1H, ArH); 7.56-7.58 (d, *J* = 8.40 Hz, 2H, ArH); 7.75-7.77 (d, *J* = 8.60 Hz, 2H, ArH); 7.81-7.83 (d, *J* = 8.40 Hz, 2H, ArH). <sup>13</sup>C NMR (DMSO-d<sub>6</sub>, 100 MHz) δ: 21.53, 43.36, 60.04, 107.91, 126.02, 126.11(2), 126.44(2), 126.57, 126.97, 127.21, 127.90, 128.49(2), 129.94(2), 138.67, 140.55, 144.25, 149.39, 153.96, 165.17. ESI-MS:

452.91(C<sub>23</sub>H<sub>19</sub>ClN<sub>3</sub>OS<sub>2</sub>, [M+H]<sup>+</sup>). Anal. Calcd for C<sub>23</sub>H<sub>18</sub>ClN<sub>3</sub>OS<sub>2</sub>: C, 61.12; H, 4.01; N, 9.30; Found: C, 61.17; H, 4.21; N, 9.37.

**4.4.20. 2-(3-(4-Chlorophenyl)-5-(thiophen-2-yl)-4,5-dihydro-1H-pyrazol-1-yl)-4-(4-(trifluoromethyl)phenyl)thiazole (10d).**

Yield 49%; mp. 209-211 °C. <sup>1</sup>H NMR (400 MHz, DMSO): δ 3.55-3.61 (m, 1H, CH<sub>2</sub>); 4.01-4.09 (m, 1H, CH<sub>2</sub>); 6.02-6.07 (m, 1H, CH); 6.99-7.01 (m, 1H, ArH); 7.28 (d, *J* = 2.80 Hz, 1H, ArH); 7.44-7.48 (m, 1H, ArH); 7.57 (d, *J* = 8.60 Hz, 2H, ArH); 7.64 (s, 1H, ArH); 7.76 (d, *J* = 8.30 Hz, 2H, ArH); 7.83 (d, *J* = 5.00 Hz, 2H, ArH); 8.04 (d, *J* = 8.00 Hz, 2H, ArH). <sup>13</sup>C NMR (DMSO-d<sub>6</sub>, 100 MHz) δ: 40.82, 59.78, 105.60, 124.22, 125.74(2), 125.96(2), 127.10, 127.54, 127.88, 128.31(2), 129.02(2), 129.55, 130.94, 134.94, 136.44, 136.74, 151.08, 152.08, 169.02. ESI-MS: 490.87 (C<sub>23</sub>H<sub>16</sub>ClF<sub>3</sub>N<sub>3</sub>S<sub>2</sub>, [M+H]<sup>+</sup>). Anal. Calcd for C<sub>23</sub>H<sub>15</sub>ClF<sub>3</sub>N<sub>3</sub>S<sub>2</sub>: C, 56.38; H, 3.09; N, 8.58; Found: C, 56.39; H, 3.19; N, 8.67.

**4.5. Antiproliferation activity**

The antiproliferative activities of the prepared compounds against MCF-7 and WM266.4 cell lines were evaluated as described elsewhere with some modifications.<sup>[30]</sup> Target tumor cell lines were grown to log phase in RPMI 1640 medium supplemented with 10% fetal bovine serum. After diluting to 2 × 10<sup>4</sup> cells per mL with the complete medium, 100 μL of the obtained cell suspension were added to each well of 96-well culture plates. The subsequent incubation was left at 37 °C, 5% CO<sub>2</sub> atmosphere for 24 h before the cytotoxicity assessments. Tested samples at pre-set concentrations were added to six wells with sorafenib as positive control. After 48 h exposure period, 40 μL of PBS containing 2.5 mg mL<sup>-1</sup> of MTT (3-(4, 5 dimethylthiazol-2-yl)-2, 5-diphenyltetrazolium bromide) were added to each well. Four hours later, 100 μL extraction solution (10% SDS-5% isobutyl alcohol-0.01 M HCl) were added. After overnight incubation at 37 °C, the optical density was measured at a wavelength of 570 nm on an ELISA microplate reader. In all experiments three replicate wells were used for each drug concentration. Each assay was carried out for at least three times.

**4.6. Kinase assay**

The BRAF enzymatic assay was described by J. Dietrich et al.<sup>[31]</sup> The assay was performed in triplicate for each tested compound in this study. Briefly, 7.5 ng Mouse Full-Length GSTtagged BRAF<sup>V600E</sup> (Invitrogen, PV3849) were pre-incubated at room temperature for 1 h with 1  $\mu$ L drug and 4  $\mu$ L assay dilution buffer. The kinase assay was initiated when 5  $\mu$ L of a solution containing 200 ng recombinant human full length, N-terminal His-tagged MEK1 (Invitrogen), 200  $\mu$ M ATP (0.8  $\mu$ Ci hot ATP), and 30 mM MgCl<sub>2</sub> in dilution buffer were added. The kinase reaction was allowed to continue at room temperature for 25 min and then quenched with 5  $\mu$ L 5  $\times$  protein denaturing buffer (LDS) solution. The protein was further denatured by heating for 5 min at 70  $^{\circ}$ C. 10  $\mu$ L of each reaction were loaded into a 15-well, 4-12% precast NuPage gel (Invitrogen) and run at 200 V, and upon completion, the front, which contained excess hot ATP, was cut from the gel and discarded. The gel was then dried and developed onto a phosphor screen. The reaction that contained no active enzyme was used as the negative control, and the reaction without inhibitor was used as the positive control.

#### 4.7. Cell apoptosis assay by flow cytometry

MCF-7 cells were seeded in 16-well plates at a density of  $1 \times 10^6$  cells/well in RPMI 1640 medium and treated with 1, 3  $\mu$ M **10d** for 48 h. Cultured cells were stained with Annexin V-FITC and propidium iodide (PI) in the dark at 4  $^{\circ}$ C for 30 min and analyzed by FACS Calibur flow cytometer (Becton Dickinson, San Jose, CA) using Cell Quest software.

#### 4.8. Docking simulations

The three-dimensional X-ray structure of BRAF<sup>V600E</sup> (PDB code: 2FB8) was chosen as the template for the modeling study of compound **10d**. The pdb file about the crystal structure of the BRAF<sup>V600E</sup> kinase domain bound to SB-590885 (2FB8.pdb) was obtained from the RCSB protein data bank (<http://www.pdb.org>). The molecular docking procedure was performed using the CDOCKER protocol for the receptor–ligand interactions section of Discovery Studio 3.5 (Accelrys Software Inc, San Diego, CA).<sup>[32,33]</sup> All bound water and ligands were eliminated from the protein and the polar hydrogen was added. The whole BRAF<sup>V600E</sup> complex was defined as a receptor and the site sphere was selected based on the ligand binding location of SB-590885,

then the SB-590885 molecule was removed and replaced with compound **10d** during the molecular docking procedure. The types of interactions of the docked protein with ligand were analyzed after the end of molecular docking.

#### 4.9. QSAR model

A series of 20 compounds was conducted as a training set for QSAR modeling. Since it is essential to assess the predictive power of the resulting QSAR models on an external set of inhibitors, 80% (that is, 16) were utilized as a training set for QSAR modeling and the remaining 20% (that is, 4) were chosen as an external test subset for validating the reliability of the QSAR model by the Diverse Molecules protocol in Discovery Studio 3.5. The selected test compounds were: **10b, 6d, 9a, 9d**.

The inhibitory abilities of the compounds in these literatures [ $IC_{50}$  (mol/L)] was changed to the minus logarithmic scale [ $pIC_{50}$  (mol/L)] and then used for subsequent QSAR analyses as the response variable.

In Discovery Studio, the CHARMM force field is used and the electrostatic potential and the van der Waals potential are treated as separate terms. A +1e point charge is used as the electrostatic potential probe and distance-dependent dielectric constant is used to mimic the solvation effect. For the van der Waals potential a carbon atom with a 1.73 Å radius is used as a probe. The truncation for both the steric and the electrostatic energies was set to 30 kcal/mol. The standard parameters implemented in Discovery Studio 3.5 were used.

A Partial Least-Squares (PLS) model is built using energy grids as descriptors. QSAR models were built using the created 3D QSAR protocol of Discovery Studio 3.5.

#### Acknowledgments

This work was supported by Natural Science Foundation of Jiangsu Province (No. BK20130554) and supported by Major Projects on Control and Rectification of Water Body Pollution (No. 2011ZX07204-001-2214 004).

## References and notes

- [1] Peyssonnaud, C.; Eychène, A. *BioL. Cell.* **2001**, *93*, 53.
- [2] Wellbrock, C.; Karasarides, M.; Marais, R. *Nat. Rev. Mol. Cell Biol.* **2004**, *5*, 875.
- [3] Gray-Schopfer, V.; Wellbrock, C.; Marais, R. *Nature.* **2007**, *445*, 851.
- [4] Davies, H.; Bignell, G. R.; Cox, C.; Stephens, P.; Edkins, S.; Clegg, S.; Teague, J.; Woffendin, H.; Garnett, M. J.; Bottomley, W.; Davis, N.; Dicks, E.; Ewing, R.; Floyd, Y.; Gray, K.; Hall, S.; Hawes, R.; Hughes, J.; Kosmidou, V.; Menzies, A.; Mould, C.; Parker, A.; Stevens, C.; Watt, S.; Hooper, S.; Wilson, R.; Jayatilake, H.; Gusterson, B. A.; Cooper, C.; Shipley, J.; Hargrave, D.; Pritchard-Jones, K.; Maitland, N.; Chenevix-Trench, G.; Riggins, G. J.; Bigner, D.D.; Palmieri, G.; Cossu, A.; Flanagan, A.; Nicholson, A.; Ho, J. W.; Leung, S. Y.; Yuen, S. T.; Weber, B. L.; Seigler, H. F.; Darrow, T. L.; Paterson, H.; Marais, R.; Marshall, C. J.; Wooster, R.; Stratton, M. R.; Futreal, P. A. *Nature.* **2002**, *417*, 949.
- [5] Tuveson, D. A.; Weber, B. L.; Herlyn, M. *Cancer Cell.* **2003**, *4*, 95.
- [6] Riesco-Eizaguirre, G.; Santisteban, P. *Endocr. Relat. Cancer.* **2007**, *14*, 957.
- [7] Li, Y.; Nakamura, M.; Kakudo, K. *Oncol. Rep.* **2009**, *22*, 671.
- [8] Tannapfel, A.; Sommerer, F.; Benicke, M.; Katalinic, A.; Uhlmann, D.; Witzigmann, H.; Hauss, J.; Wittekind, C. *Gut.* **2003**, *52*, 706.
- [9] Garnett, M. J.; Marais, R. *Cancer Cell.* **2004**, *6*, 313.
- [10] Dong, J. J.; Li, Q. S.; Wang, S. F.; Li, C. Y.; Zhao, X.; Qiu, H. Y.; Zhao, M. Y.; Zhu, H. L. *Org. Biomol. Chem.* **2013**, *11*, 6328
- [11] King, A. J.; Patrick, D. R.; Batorsky, R. S.; Ho, M. L.; Do, H. T.; Zhang, S. Y.; Kumar, R.; Rusnak, D. W.; Takle, A. K.; Wilson, D. M.; Hugger, E.; Wang, L.; Karreth, F.; Lougheed, J. C.; Lee, J.; Chau, D.; Stout, T. J.; May, E. W.; Rominger, C. M.; Schaber, M. D.; Luo, L.; Lakdawala, A. S.; Adams, J. L.; Contractor, R. G.; Smalley, K. S. Herlyn, M.; Morrissey, M.M.; Tuveson, D. A.; Huang, P. S. *Cancer Res.* **2006**, *66*, 11100.
- [12] McDermott, U.; Sharma, S. V.; Dowell, L.; Greninger, P.; Montagut, C.; Lamb, J.; Archibald, H.; Raudales, R.; Tam, A.; Lee, D.; Rothenberg, S. M.; Supko, J. G.; Sordella, R.; Ulkus, L. E.; Iafrate, A. J.; Maheswaran, S.; Njauw, C. N.; Tsao, H.; Drew, L.; Hanke, J. H.; Ma, X. J.; Erlander, M. G.; Gray, N. S.; Haber, D. A.; Settleman, J. *Proc. Natl. Acad. Sci. U. S. A.* **2007**, *104*, 19936.

- [13] Flaherty, K. T.; Puzanov, I.; Kim, K. B.; Ribas, A.; McArthur, G. A.; Sosman, J. A.; O'Dwyer, P. J.; Lee, R. J.; Grippo, J. F.; Nolop, K.; Chapman, P. B. *N. Engl. J. Med.* **2010**, *363*, 809.
- [14] Roberts, P. J.; Der, C. J. *Oncogene.* **2007**, *26*, 3291.
- [15] Bollag, G.; Hirth, P.; Tsai, J.; Zhang, J.; Ibrahim, P. N.; Cho, H.; Spevak, W.; Zhang, C.; Zhang, Y.; Habets, G.; Burton, E. A.; Wong, B.; Tsang, G.; West, B. L.; Powell, B.; Shellooe, R.; Marimuthu, A.; Nguyen, H.; Zhang, K. Y.; Artis, D. R.; Schlessinger, J.; Su, F.; Higgins, B.; Iyer, R.; D'Andrea, K.; Koehler, A.; Stumm, M.; Lin, P. S.; Lee, R. J.; Grippo, J.; Puzanov, I.; Kim, K. B.; Ribas, A.; McArthur, G. A.; Sosman, J. A.; Chapman, P. B.; Flaherty, K. T.; Xu, X.; Nathanson, K. L.; Nolop, K. *Nature*, **2010**, *467*, 596.
- [16]: Wang, J.; Chen, J. J.; Miller, D. D.; Li, W. *Mol. Cancer. Ther.* **2014**, *13*, 16.
- [17] Zambon, A.; Ménard, D.; Suijkerbuijk, B. M.; Niculescu-Duvaz, I.; Whittaker, S.; Niculescu-Duvaz, D.; Nourry, A.; Davies, L.; Manne, H. A.; Lopes, F.; Preece, N.; Hedley, D.; Ogilvie, L. M.; Kirk, R.; Marais, R.; Springer, C. J. *J. Med. Chem.* **2010**, *53*, 5639.
- [18] Li, C.Y.; Li, Q. S.; Yan, L.; Sun, X.G.; Wei, R.; Gong, H. B.; Zhu, H. L. *Bioorg. Med. Chem.* **2012**, *20*, 3746.
- [19] Barsoum, F. F.; Hosni, H. M.; Girgis, A. S; *Bioorg. Med. Chem.* **2006**, *14*, 3929.
- [20] De, D.; Krogstad, F. M.; Byers, L. D.; Krogstad, D. J. *J. Med. Chem.* **1998**, *41*, 4918.
- [21] Ghorab, M. M.; Ragab, F. A.; Alqasoumi, S. I.; Alafeefy, A. M.; Aboulmagd, S. A. *Eur. J. Med. Chem.* **2010**, *45*, 171.
- [22] Lu, Y.; Li, C. M.; Wang, Z.; Ross, C. R.; Chen, J.; Dalton, J. T.; Miller, D. D. *J. Med. Chem.* **2009**, *52*, 1701.
- [23] Höfle, G.; Glaser, N.; Leibold, T.; Sefkow, M. *Pure. Appl. Chem.* **1999**, *71*, 2019.
- [24] Nieves-Neira, W.; Rivera, M. I.; Kohlhagen, G.; Hursey, M. L.; Pourquier, P.; Sausville, E. A.; Pommier, Y. *Mol. Pharmacol.* **1999**, *56*, 478.
- [25] Flynn, B. L.; Flynn, G. P.; Hamel, E.; Jung, M. K. *Bioorg. Med. Chem. Lett.* **2001**, *11*, 2341.
- [26] Al-Said, M. S.; Bashandy, M. S.; Al-Qasoumi, S. I.; Ghorab, M. M. *Eur. J. Med. Chem.* **2011**, *46*, 137.
- [27] Said, M.; Elshihawy, H. *Pak. J. Pharm. Sci.* **2014**, *27*, 885.
- [28] Dallemagne, P.; Khanh, L. P.; Alsaïdi, A.; Renault, O.; Varlet, I.; Collot, V.; Bureau, R.; Rault, S. *Bioorg. Med. Chem.* **2002**, *10*, 2185.

- [29] Shams, H. Z.; Mohareb, R. M.; Helal, M. H.; Mahmoud, A. E. *Molecules*. **2010**, *16*, 52.
- [30] Wu, G.; Robertson, D. H.; Brooks, C. L.; Vieth, M. J. *Comput. Chem.* **2003**, *24*, 1549.
- [31] Boumendjel, A.; Boccard, J.; Carrupt, P. A.; Nicolle, E.; Blanc, M.; Geze, A.; Choisnard, L.; Wouessidjewe, D.; Matera, E. L.; Dumontet, C. *J. Med. Chem.* **2008**, *51*, 2307.
- [32] Dietrich, J.; Hulme, C.; Hurley, L. H. *Bioorg. Med. Chem.* **2010**, *18*, 5738.
- [33] Roy, U.; Sokolowska, I.; Woods, A. G.; Darie, C. C. *Biotechnol. Appl. Bioc.* **2012**, *59*, 445.

ACCEPTED MANUSCRIPT

**Figure captions**

**Scheme 1.** Synthesis of compound **6a-10d**. Reagents and conditions: (i) ethanol, 25 °C, 10 minutes; (ii) thiosemicarbazide EtOH, reflux, 2h; (iii) DMF, 25 °C.

**Table 1.** Inhibition ( $IC_{50}$ ) of MCF-7 and WM266.4 cells proliferation and inhibition of BRAF<sup>V600E</sup> by compounds **6a-10d** ( $\mu$ M).

**Table 2.** Binding energy of compounds **6a-10d** with BRAF<sup>V600E</sup>.

**Table 3.** Experimental, predicted inhibitory activity of compounds **6a-10d** by 3D-QSAR models based upon active conformation achieved by molecular docking.

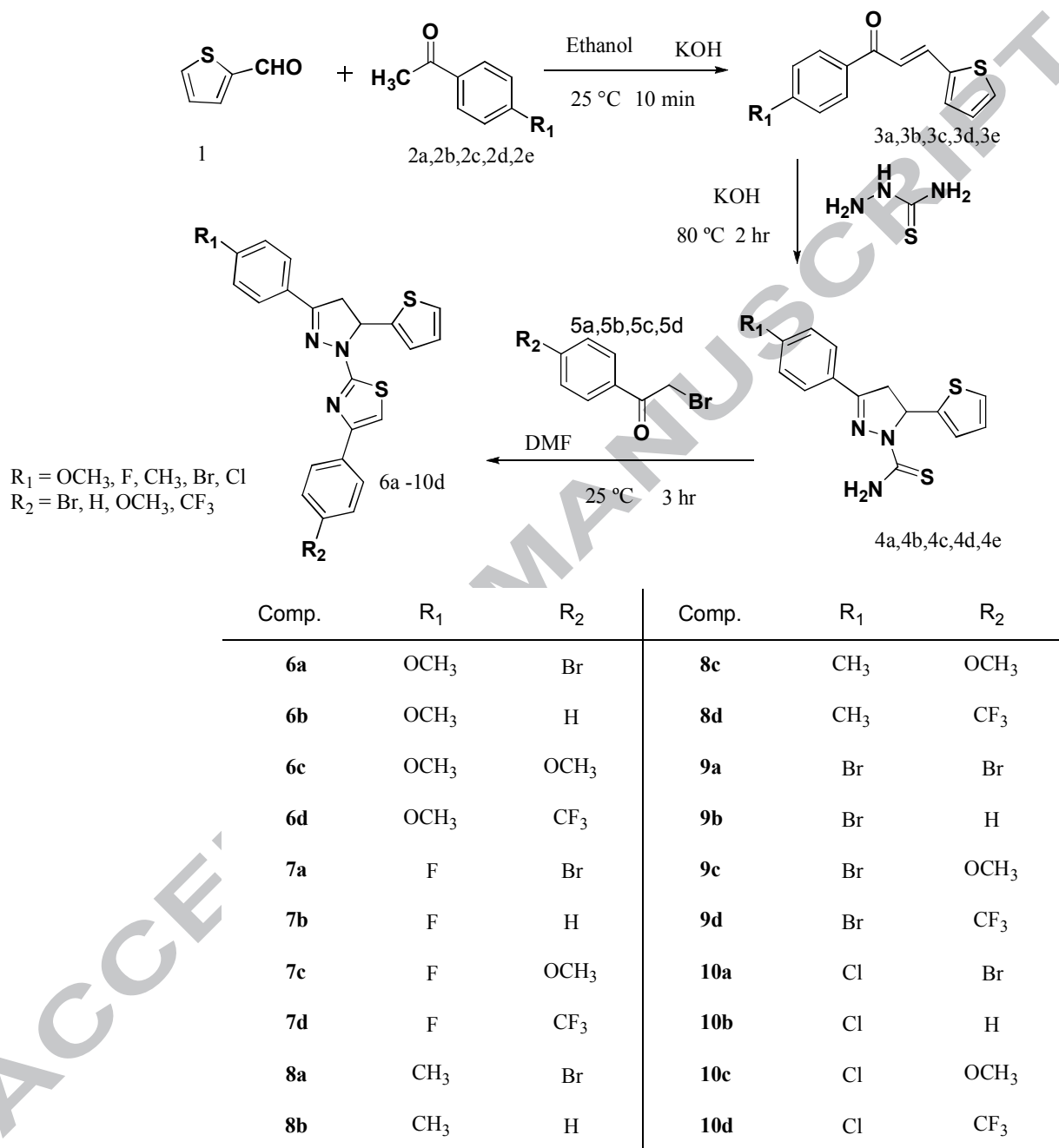
**Figure 1.** Apoptosis result by flow cytometry method of operation.

**Figure 2.** 2D binding model of compound **10d** into the active pocket of BRAF<sup>V600E</sup>.

**Figure 3.** 3D binding model of compound **10d** into the active pocket of BRAF<sup>V600E</sup>.

**Figure 4.** Plot of experimental versus predicted BRAF inhibitory activities of training set and test set.

**Figure 5.** (a) 3D-QSAR model coefficients on electrostatic potential grids. Blue represents positive coefficients; red represents negative coefficients. (b) 3D-QSAR model coefficients on van der Waals grids. Green represents positive coefficients; yellow represents negative coefficients.



**Scheme 1.** Synthesis of compound **6a-10d**. Reagents and conditions: (i) ethanol, 25 °C, 10 minutes; (ii) thiosemicarbazide EtOH, reflux, 2h; (iii) DMF, 25 °C.

**Table 1.** Inhibition (IC<sub>50</sub>) of MCF-7 and WM266.4 cells proliferation and inhibition of BRAF<sup>V600E</sup> by compounds **6a-10d** (μM).

Compound	R <sub>1</sub>	R <sub>2</sub>	IC <sub>50</sub> ± SD (μM)		
			BRAF <sup>V600E</sup>	WM266.4 <sup>a</sup>	MCF-7 <sup>a</sup>
<b>6a</b>	OCH <sub>3</sub>	Br	4.01±0.13	5.87±0.49	21.17.17±0.67
<b>6b</b>	OCH <sub>3</sub>	H	1.11±0.21	2.12±0.32	9.01±0.83
<b>6c</b>	OCH <sub>3</sub>	OCH <sub>3</sub>	5.23±0.31	31.60±1.12	16.19±0.76
<b>6d</b>	OCH <sub>3</sub>	CF <sub>3</sub>	10.90±0.56	8.11±0.78	45.67±1.01
<b>7a</b>	F	Br	1.86±0.11	0.22±0.03	8.28±0.57
<b>7b</b>	F	H	0.67±0.03	0.17±0.02	2.34±0.31
<b>7c</b>	F	OCH <sub>3</sub>	5.12±0.32	4.42±0.45	14.16±0.45
<b>7d</b>	F	CF <sub>3</sub>	1.01±0.09	5.12±0.39	1.33±0.11
<b>8a</b>	CH <sub>3</sub>	Br	0.56±0.06	18.36±1.15	2.01±0.09
<b>8b</b>	CH <sub>3</sub>	H	3.88±0.27	7.52±0.58	18.56±0.32
<b>8c</b>	CH <sub>3</sub>	OCH <sub>3</sub>	0.11±0.01	3.77±0.44	4.77±0.39
<b>8d</b>	CH <sub>3</sub>	CF <sub>3</sub>	6.18±0.07	2.11±0.26	31.48±0.79
<b>9a</b>	Br	Br	8.87±0.45	12.98±0.89	28.29±0.61
<b>9b</b>	Br	H	2.19±0.23	1.87±0.21	6.79±0.41
<b>9c</b>	Br	OCH <sub>3</sub>	0.08±0.01	2.01±0.19	0.68±0.02
<b>9d</b>	Br	CF <sub>3</sub>	2.09±0.02	27.38±0.81	7.81±0.51
<b>10a</b>	Cl	Br	4.78±0.04	1.45±0.22	14.67±0.61
<b>10b</b>	Cl	H	0.09±0.01	2.19±0.34	0.19±0.01
<b>10c</b>	Cl	OCH <sub>3</sub>	0.19±0.02	1.31±0.17	2.48±0.02
<b>10d</b>	Cl	CF <sub>3</sub>	0.05±0.01	0.12±0.01	0.16±0.01
<b>Sorafenib<sup>b</sup></b>			0.03±0.005	0.06±0.01	0.19±0.02

<sup>a</sup> BRAF<sup>V600E</sup> cell lines.<sup>b</sup> Used as a positive control.

**Table 2.** Binding energy of compounds **6a-10d** with BRAF<sup>V600E</sup>.

Comp.	Binding energy $\Delta G_b$	Comp.	Binding energy $\Delta G_b$
<b>6a</b>	-42.7731	<b>8c</b>	-41.7160
<b>6b</b>	-44.5859	<b>8d</b>	-42.8494
<b>6c</b>	-45.2577	<b>9a</b>	-44.7631
<b>6d</b>	-44.3719	<b>9b</b>	-41.6707
<b>7a</b>	-41.0285	<b>9c</b>	-42.8896
<b>7b</b>	-41.0247	<b>9d</b>	-43.0418
<b>7c</b>	-41.6267	<b>10a</b>	-44.2035
<b>7d</b>	-42.6731	<b>10b</b>	-43.5537
<b>8a</b>	-42.7915	<b>10c</b>	-41.8499
<b>8b</b>	-42.7272	<b>10d</b>	-45.6649

**Table 3** Experimental, predicted inhibitory activity of compounds **6a –10d** by 3D-QSAR models based upon active conformation achieved by molecular docking

Compound	BRAFF <sup>V600E</sup>		Residual error
	Experimental pIC <sub>50</sub>	Predicted pIC <sub>50</sub>	
<b>6a</b>	4.674	4.583	0.091
<b>6b</b>	5.045	5.068	-0.023
<b>6c</b>	4.791	4.713	0.078
<b>6d</b>	4.340	4.754	-0.414
<b>7a</b>	5.082	5.069	0.012
<b>7b</b>	5.361	5.371	-0.010
<b>7c</b>	4.849	4.875	-0.026
<b>7d</b>	5.876	5.907	-0.031
<b>8a</b>	5.696	5.602	0.094
<b>8b</b>	4.736	4.787	-0.051
<b>8c</b>	5.321	5.353	-0.032
<b>8d</b>	4.502	4.473	0.029
<b>9a</b>	4.548	5.476	-0.928
<b>9b</b>	5.168	5.277	-0.109
<b>9c</b>	6.167	6.164	0.003
<b>9d</b>	5.107	5.141	-0.034
<b>10a</b>	4.834	4.888	-0.054
<b>10b</b>	6.721	5.393	1.327
<b>10c</b>	5.606	5.622	-0.016
<b>10d</b>	6.796	6.751	0.045

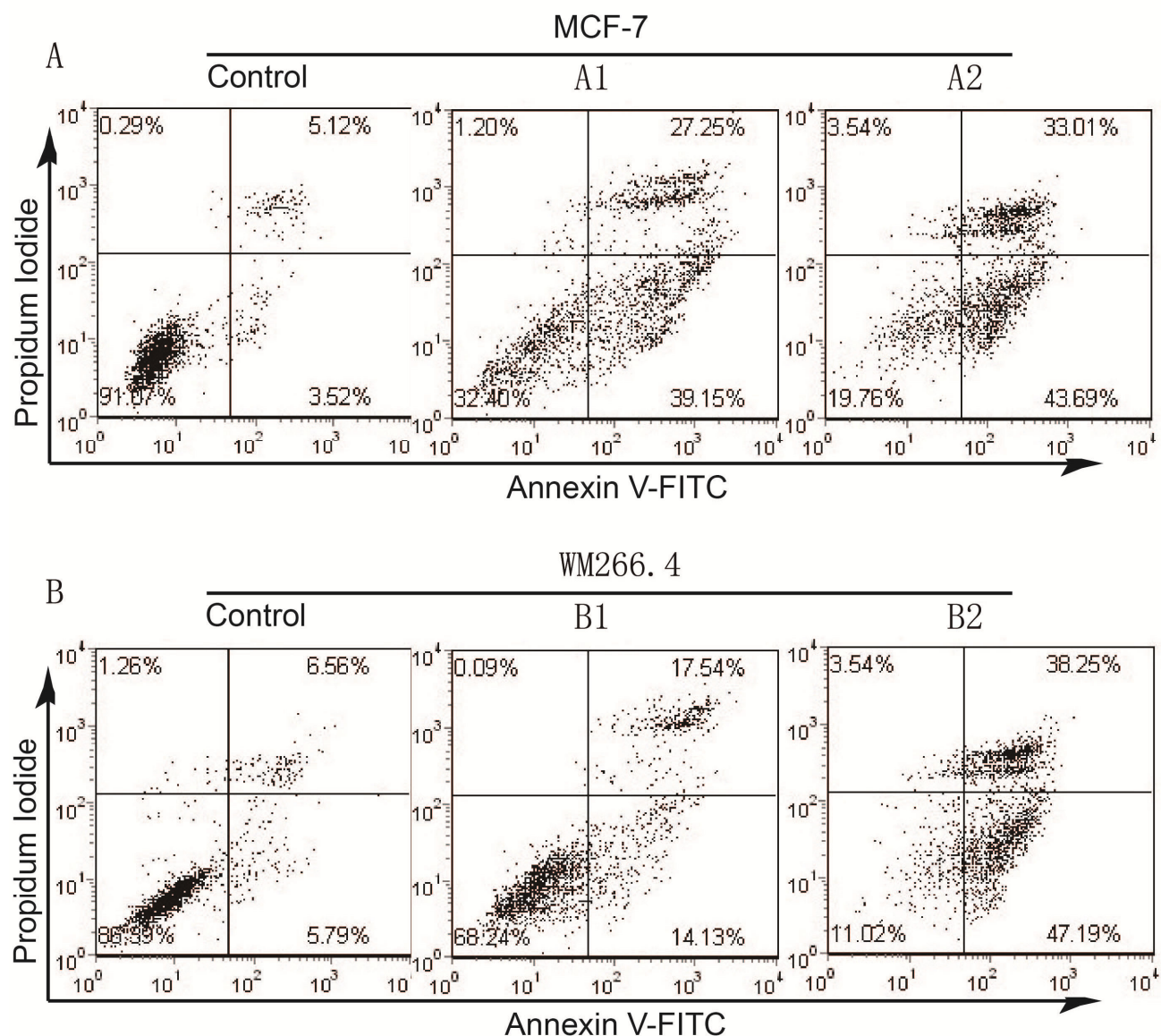


**Figure 1.** Apoptosis result by flow cytometry method of operation. The apoptosis qualitative effect was demonstrated in this two group of figures. A and B respectively represents the apoptosis qualitative effect of MCF-7 and WM 266.4 conducted by compound **10d**, which contains control group. A1, B1 equally were conducted with 1  $\mu$ M and A2, B2 were equally conducted with 3  $\mu$ M. With the dose of compound **10d** increasing, the WM 266.4 and MCF-7 were dyed more and more Propidium Iodide and Annexin V-FITC, which indicated more and more cancer cell gradually encountered apoptosis or died. When conducted with 3  $\mu$ M, most of the WM 266.4 and MCF-7 were caught in apoptosis and even died. This result explains compound **10d** could induce the apoptosis of MCF-7 and WM266.4 by qualitative analysis.

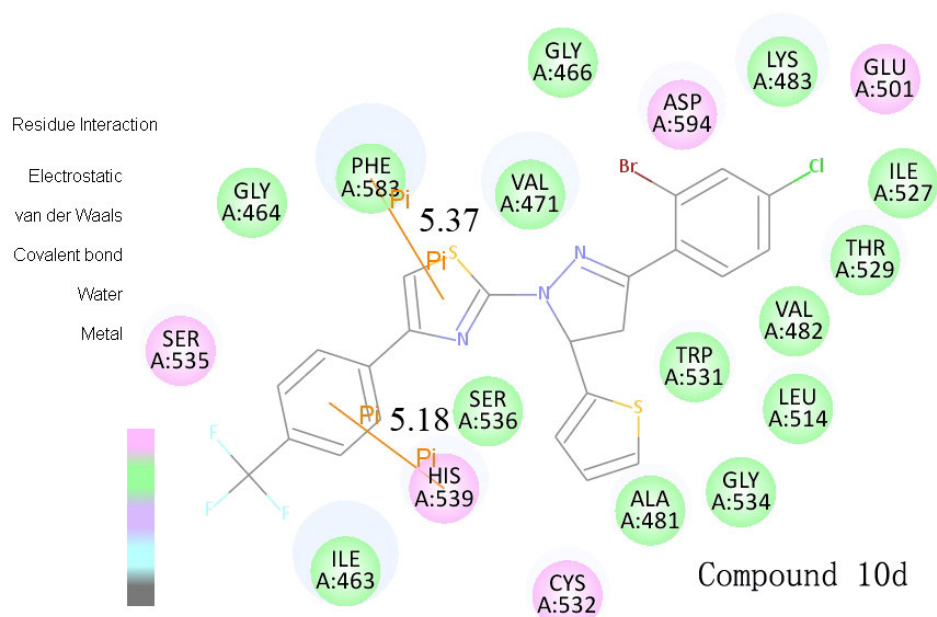


**Figure 2.** 2D binding model of compound **10d** into the active pocket of BRAF<sup>V600E</sup>

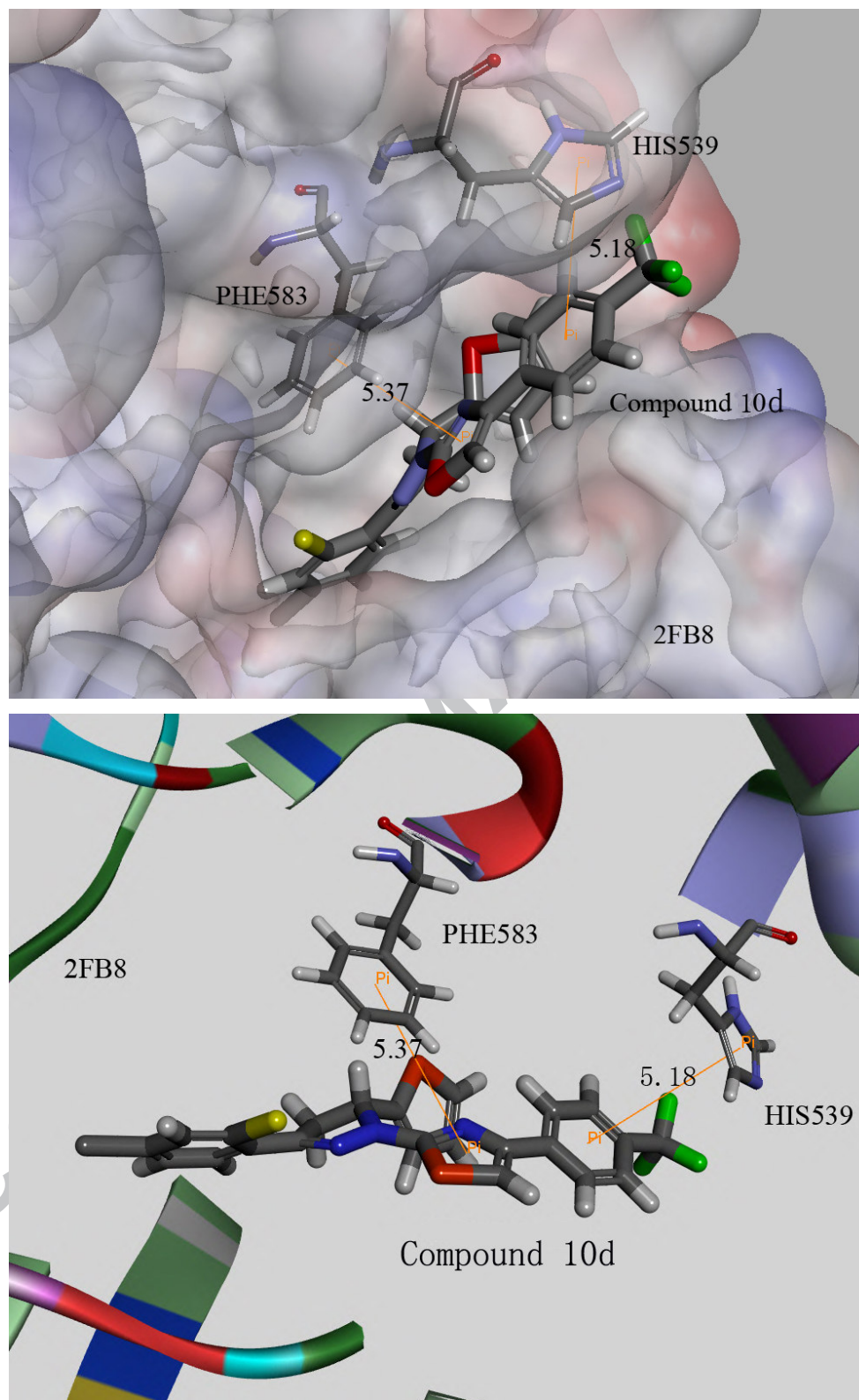


**Figure 3.** 3D binding model of compound **10d** into the active pocket of BRAF<sup>V600E</sup>.

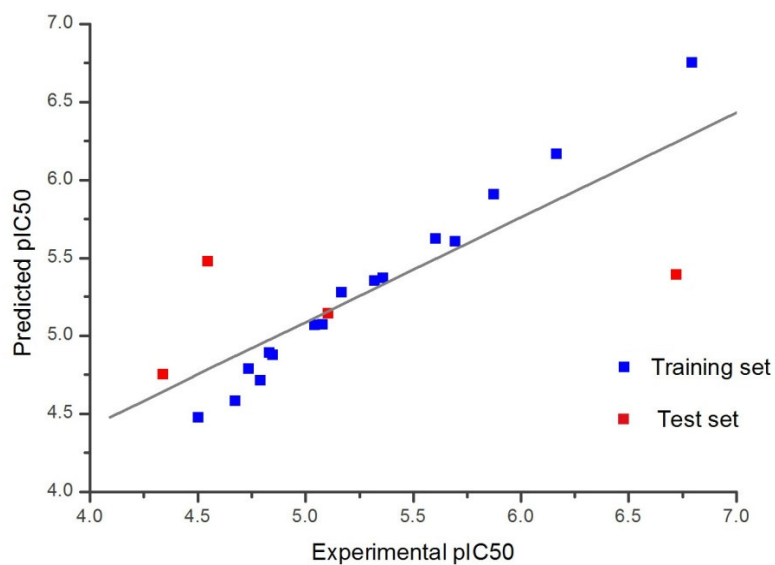


**Figure 4.** Plot of experimental versus predicted BRAF inhibitory activities of training set and test set.

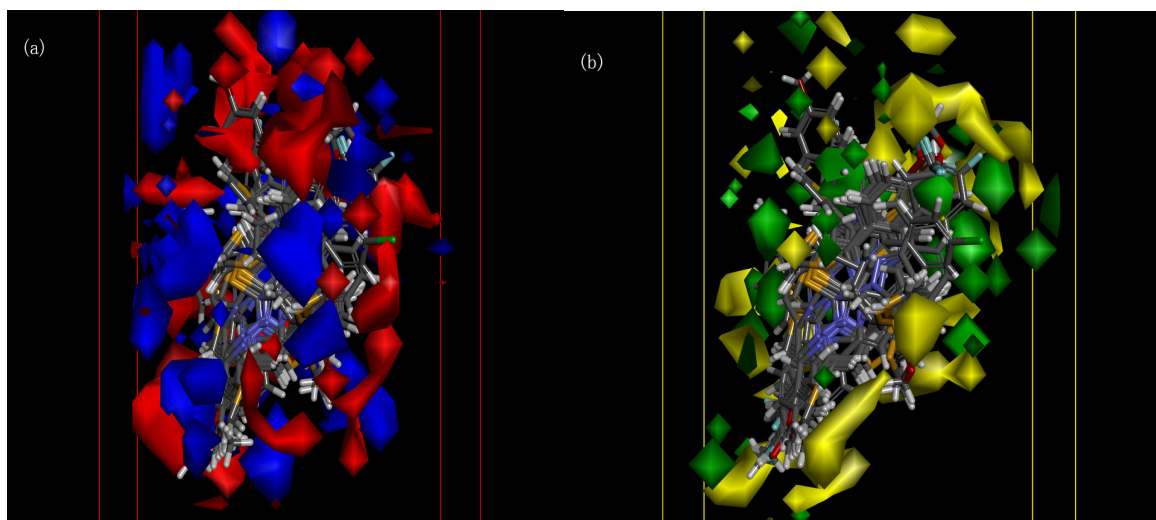


**Figure 5.** (a) 3D-QSAR model coefficients on electrostatic potential grids. Blue represents positive coefficients; red represents negative coefficients. (b) 3D-QSAR model coefficients on van der Waals grids. Green represents positive coefficients; yellow represents negative coefficients.

**Synthesis, biological evaluation and 3D-QSAR study of novel 4, 5-dihydro-1H-pyrazole  
thiazole derivatives as BRAF<sup>V600E</sup> inhibitors**

Meng-Yue Zhao<sup>+a</sup>, Yong Yin<sup>+a</sup>, Xiao-Wei Yu<sup>a</sup>, Chetan B. Sangani<sup>a</sup>, Shu-Fu Wang<sup>a</sup>, Ai-Min Lu<sup>b</sup>, Li-Fang Yang<sup>ac</sup>, Peng-Cheng Lv<sup>\*a</sup>, Ming-Guo Jiang<sup>\*ac</sup>, Hai-Liang Zhu<sup>\*a</sup>

<sup>a</sup> State Key Laboratory of Pharmaceutical Biotechnology, Nanjing University, Nanjing 210093,  
People's Republic of China

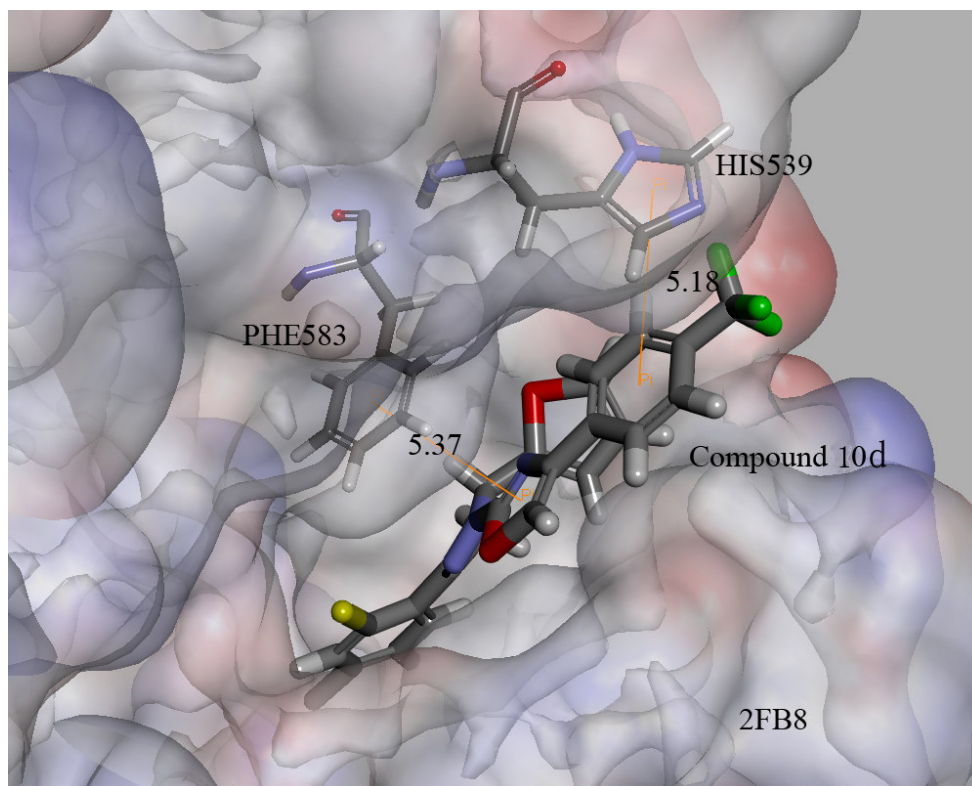
<sup>b</sup> College of Science, Nanjing Agriculture University, Nanjing 210095, People's Republic of China

<sup>c</sup> Guangxi Colleges and Universities Key Laboratory of Utilization of Microbial and Botanical Resources, Guangxi University for nationalities, 530006

<sup>+</sup> These authors contributed equally to this work.

<sup>\*</sup> Corresponding authors. Tel.: +86 25 83592572; Fax: +86 25 83592672.

E-mail address: zhuhl@nju.edu.cn (H.-L. Zhu).



To provide new therapeutic opportunities, a series of novel 4,5-dihydro-1*H*-pyrazole derivatives (**6a-10d**) containing thiazole moiety as potential V600E mutant BRAF kinase (BRAF<sup>V600E</sup>) inhibitors were designed and synthesized. All compounds were evaluated *in vitro* for anticancer activities against WM266.4 and MCF-7 cell line. Compound **10d** displayed the most potential antiproliferative activity.